Monitoring Drug-Protein Interactions in the Bacterial Periplasm by Solution Nuclear Magnetic Resonance Spectroscopy

Alicja Razew, Quentin Herail, Mayara Miyachiro, Constantin Anoyatis-Pelé, Catherine Bougault, Andrea Dessen, Michel Arthur, Jean-Pierre Simorre

▶ **To cite this version:**

Alicja Razew, Quentin Herail, Mayara Miyachiro, Constantin Anoyatis-Pelé, Catherine Bougault, et al.. Monitoring Drug-Protein Interactions in the Bacterial Periplasm by Solution Nuclear Magnetic Resonance Spectroscopy. Journal of the American Chemical Society, In press, 10.1021/jacs.4c00604 . hal-04510786

HAL Id: hal-04510786
https://cnrs.hal.science/hal-04510786v1

Submitted on 19 Mar 2024

HAL is a multi-disciplinary open access archive for the deposit and dissemination of scientific research documents, whether they are published or not. The documents may come from teaching and research institutions in France or abroad, or from public or private research centers.

L'archive ouverte pluridisciplinaire **HAL**, est destinée au dépôt et à la diffusion de documents scientifiques de niveau recherche, publiés ou non, émanant des établissements d'enseignement et de recherche français ou étrangers, des laboratoires publics ou privés.

Monitoring Drug-Protein Interactions in the Bacterial Periplasm by Solution Nuclear Magnetic Resonance Spectroscopy

Alicja Razew[a], Quentin Herail[b], Mayara Miyachiro[a†], Constantin Anoyatis-Pelé[b], Catherine Bougault[a], Andrea Dessen[a], Michel Arthur[b], Jean-Pierre Simorre[a*]

[a]*Université Grenoble Alpes, CNRS, CEA, Institut de Biologie Structurale, Grenoble, 38044, France*

[b]*INSERM, Sorbonne Université, Université Paris Cité, Paris, 75006, France*

KEYWORDS: Nuclear magnetic resonance, in-cell, beta-lactamases, penicillin-binding proteins, antibiotic resistance

ABSTRACT: Rapid spread of antimicrobial resistance across bacterial pathogens poses a serious risk to the efficacy and sustainability of available treatments. This puts pressure on research concerning development of new drugs. Here, we present an in-cell NMR-based research strategy to monitor the activity of the enzymes located in the periplasmic space delineated by the inner and outer membranes of Gram-negative bacteria. We demonstrate its unprecedented analytical power in monitoring *in situ* and in a real time (i) the hydrolysis of β-lactams by β-lactamases, (ii) the interaction of drugs belonging to the β-lactam family with their essential targets, and (iii) the binding of inhibitors to these enzymes. We show that in-cell NMR provides a powerful analytical tool for investigating new drugs targeting molecular components of the bacterial periplasm.

INTRODUCTION

Bacteria use multiple means to resist to the action of antibiotics[1]. Among them, a key response employed by Gram-negative pathogens is the enzymatic hydrolysis of β-lactams[2,3]. These antibiotics irreversibly inactivate the essential penicillin-binding proteins (PBPs) that perform the last cross-linking step of cell wall peptidoglycan (PG) biosynthesis. Acylation of the active-site serine nucleophile of these PBPs leads to their inactivation and triggers the cascade of events leading to bacterial cell death[4,5]. Most bacteria classified by WHO as critical priorities for the development of new drugs produce β-lactamases of broad spectrum substrate specificity that hydrolyze β-lactams belonging to the cephalosporin or carbapenem classes, or both[1]. Although β-lactamase inhibitors have been successfully developed in order to restore the activity of β-lactams against resistant bacteria, they do not cover the wide variety of β-lactamases produced by Gram-negative bacteria, in particular the class B metallo-enzymes[6]. The currently available inhibitors belong to three chemical classes based on β-lactam (clavulanate), diazabicyclooctane (avibactam), and boronate (vaborabactam) scaffolds[7].

The study of the mode of action and efficacy of β-lactams and β-lactam/β-lactamase inhibitor combinations are highly complex because the drugs competitively interact with multiple enzymes in the bacterial periplasm. Critical reactions are triggered by (i) competitive binding of β-lactams to PBPs or to β-lactamases leading to irreversible target or β-lactam inactivation, (ii) competitive binding of β-lactams or β-lactamase inhibitors to β-lactamases leading to β-lactam inhibition or β-lactamase inactivation, and (iii) competitive binding of β-lactams or PG precursors to PBPs leading to target inactivation or PG cross-linking.[8] An additional level of complexity arises from the fact that the reactions catalyzed by PBPs are performed by multiple enzymes with partially redundant functions for which currently available assays based on purified enzymes do not recapitulate the catalytic efficacies required to sustain PG polymerization in their physiological periplasmic environment, in particular for class B PBPs[9–11]. In fact *in vitro* assays showed that polymerization of glycan chains is a prerequisite for transpeptidation. For this reason, these assays are based on the synthesis and purification of the substrate of the glycosyltransferases, *i.e.* the full disaccharide-peptide PG subunit linked to the undecaprenyl lipid carrier (lipid II), which is difficult to obtain. In addition, protein cofactors need to be incorporated into the assays for optimal PBP activity. As a result, the complexity of the *in vitro* PG polymerization assays severely limits the evaluation of β-lactam efficacy based on inhibition of the catalytic activity of PBPs. Thus, our understanding of the mode of action of β-lactams and the identification of the drug properties that should be improved to counteract resistance mechanisms will benefit from experimental approaches enabling to simultaneously monitor the fate of β-lactams, β-lactamase inhibitors, and of β-lactam-interacting proteins in the bacterial periplasm. The drug properties that should be considered for improving drug efficacy against resistant strains include their capacity to rapidly and irreversibly inactivate PBPs, to escape hydrolysis by β-lactamases, and to effectively translocate across the outer membrane of Gram-negative bacteria. Absorbance and fluorescence spectroscopies are generally used to explore the efficacy of PBP inactivation by β-lactams using purified enzymes. These spectroscopic approaches provide the kinetic data required to explore the reaction paths leading to PBP acylation by β-lactams or to β-lactam hydrolysis by β-lactamases using assays containing a single enzyme. However, these approaches cannot resolve multiple drug-target interactions in competitive reactions (reactions i to iii, above) because rupture of the β-lactam ring upon target acylation or drug hydrolysis results in similar

decreases in absorbance. Moreover, tryptophan fluorescence quenching occurs both for PBPs and β-lactamases[12]. The current study explores the use of NMR to fill this methodology gap.

In recent years, we have observed the advent of *in situ* structural biology approaches that enable us to study molecular machines directly in their native, complex environment[13–15]. One of the quickly expanding fields in this context is in-cell (or in situ) NMR leveraged for studies on structural and functional features of proteins and other macromolecules determined directly in living bacterial and eukaryotic cells. It proved paricuoarly useful to follow cellular organization (*e.g.* structure of cell walls and membranes), metabolism (turnover, metabolic pathways elucidation), drug action in time-resolved experiments (screening, mode of action) or evolution of local chemical environment (pH, viscosity, homogeneity) directly in physiological conditions and at atomic resolution [16–18].

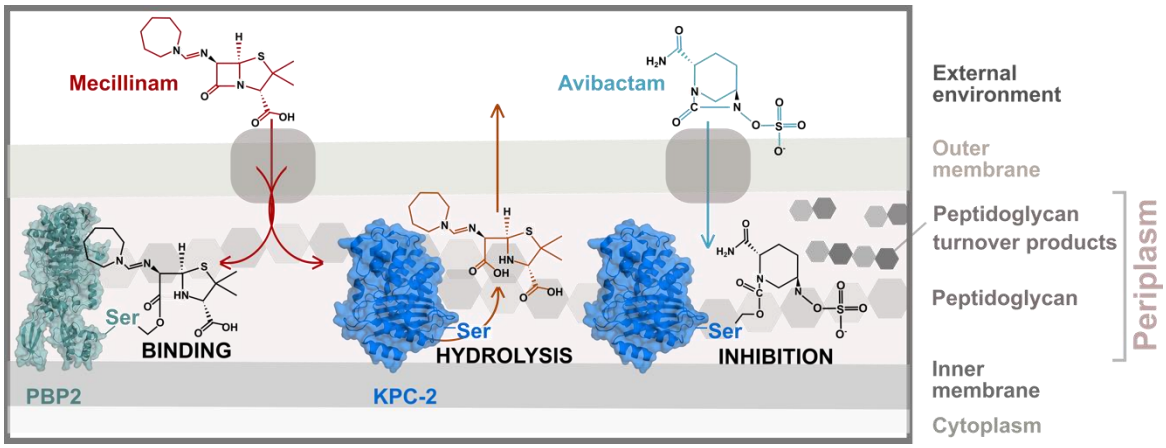

Scheme 1. Cell envelope of Gram-negative bacteria and drug-protein interactions monitored in this work

Here, we explore the possibility of using in-cell NMR to characterize the bacterial periplasm, the cellular compartment at the frontline of drug passage and/or accumulation, in definite drug-target and drug-β-lactamase interactions (**Scheme 1**). We optimized experimental conditions for recording NMR spectra of the carbapenemase KPC-2 *in situ*, which further served to follow chemical shift perturbations (CSPs) caused by the interaction of this β-lactamase with avibactam, the prototypic inhibitor of the diazabicyclooctane family. To complete the picture, we identified specific PG turnover products, that accumulate in response to peptidoglycan cross-linking inhibition by β-lactams[19,20] and additionally act as a molecular signal for β-lactamase induction in most enterobacteria and in *Pseudomonas aeruginosa*[21]. Therefore, the capacity to monitor PG recycling is a way to characterize the effect of new antibiotics on bacterial physiology and resistance onset. Finally, we demonstrate that our experimental setup enables tracking the activity of β-lactamases on β-lactams and distinguishing this activity from PBP inactivation without selective labelling of β-lactamases or PBPs. In all, we present here a comprehensive set of in-cell NMR experiments, providing a methodological toolkit for antimicrobial research.

RESULTS AND DISCUSSION

Periplasmic PG fragments and proteins are observable *in situ*

Our first objective was to determine whether NMR could be used to identify periplasmic components in entire bacterial cells. To this end, we performed 2D ^{1}H-^{15}N SOFAST experiments[22] at 37°C using, as a model of resistant Gram-negative bacteria, *Escherichia coli* cells producing KPC-2, following cloning of the corresponding gene under the control of an IPTG-inducible promoter. KPC-2 is a periplasmic enzyme and a member of the most prevalent family of class A carbapenemases[13]. The cells were embedded in PBS solidified with agar (0.5%). This optimized agar concentration prevents cell aggregation during long-term NMR experiments and enables collecting signal of high quality due to the optimal cell density and sample viscosity (**Figure 1a, Figure S1**).

Firstly, we noticed the presence of amide resonances that could correspond to peptidoglycan (PG) fragments, termed muropeptides (**Figure 1b**). These products are extractable in the soluble periplasmic fraction (**Figure S2a**), which allowed us to discriminate them from the insoluble PG macromolecule of the native cell wall. To further characterize the structure of the putative periplasmic muropeptides, we isolated PG from *E. coli* cultured in M9 medium supplemented with ^{13}C- and ^{15}N-uniformly labelled carbon and ammonium sources. PG was then digested with a muramidase (mutanolysin) (**Figure S2b**), which cleaves β-(1→4) glycosidic bonds connecting *N*-acetylmuraminyl (MurNAc) to *N*-acetylglucosaminyl (GlcNAc) residues. The resulting soluble disaccharide-peptide fragments were subjected to specific NMR resonance assignment. Amide resonances showed a very nice dispersion and a high sensitivity to the chemical environment of each amino acid or *N*-acetylated saccharide (**Figure S3**). 3D backbone and side-chain NMR sequences developed for protein NMR and 3D HCCH-TOCSY experiments were adapted to assign ^{1}H, ^{13}C and ^{15}N resonances of each amino acid in dedicated peptide stems and of each saccharide, respectively (**Figure S3-S5**). Starting from the C-terminal end of each peptide stem, we could differentiate amide resonances of muropeptide monomers composed of the GlcNAc-

MurNAc disaccharide and a tetrapeptide stem linked to MurNAc, *i.e.*, uncross-linked muropeptides, from muropeptide dimers resulting from the cross-linking of two disaccharide-peptides by PBPs (**Figure 1b, Figure S3**)[23]. These muropeptides contained both the α and β anomers of MurNAc, which were identified from the unique chemical shift signature of the resonance from the anomeric positions (**Figure S5**)[24]. Corresponding assignments (**Table S1**) were then transferred to muropeptide NMR spectra collected in the temperature, buffer and pH experimental conditions used for in-cell and periplasmic extract analyses. The amide resonances identified in the in-cell spectrum and in the mutanolysin digest extensively overlapped, allowing further assignment transfer (**Figure S2a**). In addition, we also detected NMR peaks corresponding to 1,6-anhydro-*N*-acetylmuramyl residues (anhMurNAc). These residues result from digestion of PG by lytic transglycosylases which cleave the β-(1→4) MurNAc-GlcNAc bond with simultaneous cyclisation in the terminal MurNAc to form 1,6-anhydroMurNAc. These periplasmic anhydro muropeptides were identified based on the overlap in amide resonances recorded after digestion of PG with purified lytic transglycosylase MltG and on the comparison to the mutanolysin digest (**Figure S2).** The presence of anhydro muropeptides was expected because PG turnover and recycling is thought to be mainly meditated by lytic transglycosylases[25]. Accordingly, in-cell signals of α-MurNAc and β-MurNAc *versus* anhMurNAc were detected at an intensity ratio of 5 to 1. These results show that short specific periplasmic PG fragments are NMR observable *in situ*.

Secondly, we sought to identify amide resonances corresponding to periplasmic KPC-2 in whole cells. The activity of KPC-2 was assessed by measuring changes in light absorbance resulting from hydrolysis of the chromogenic cephalosporin nitrocefin by periplasmic extracts isolated from *E. coli* cultures (**Figure 1c**). It confirmed that *E. coli* produced KPC-2 in an IPTG-inducible manner. The ^{1}H protein amide resonances are well resolved in the region between 9 and 11 ppm, and overlap partially in the 7.9-8.6 ppm region that contains intrinsically disordered proteins (IDPs) signals (**Figure 1a**)[26]. To filter out signals not originating from KPC-2 amide resonances, we subtracted experiments recorded without expression of the gene encoding KPC-2 from experiments recorded with expression of this gene. This subtraction process efficiently filtered out non KPC-2 signals, *i.e.* signals from IDPs and muropeptides, and provided an enhanced visualization of the KPC-2 ^{1}H-^{15}N correlation spectrum (**Figure 1d, Figure S6**)[27].

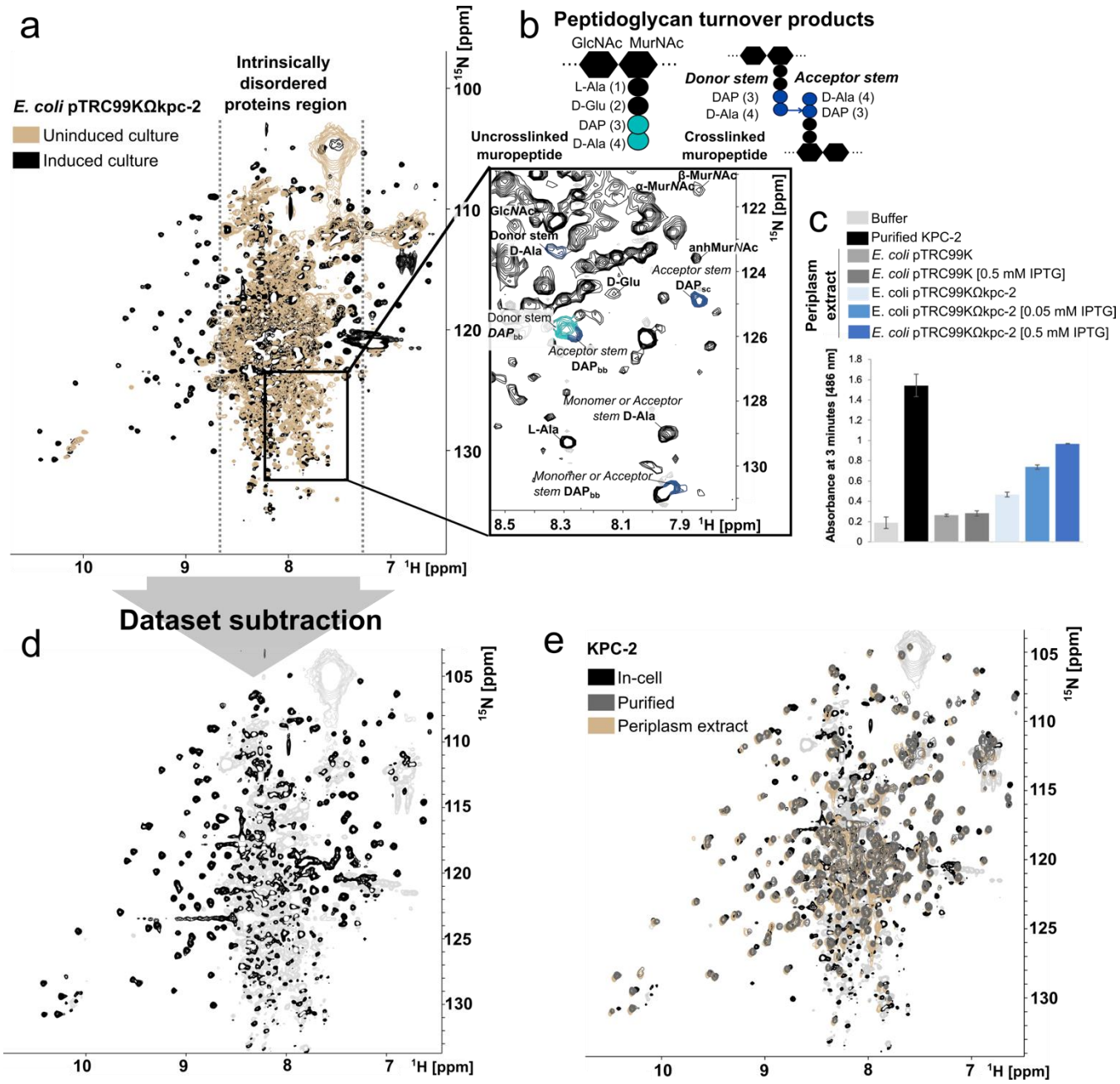

Figure 1 Periplasm components are observable *in situ*

a. 2D ^{1}H-^{15}N correlation spectra recorded for 14 h at 37 °C and pH 7.4 on a 950 MHz spectrometer for *E. coli* pTRC99KΩ*kpc-2* not induced (wheat) and induced with 1 mM IPTG (black). Dashed lines indicate the region corresponding to intrinsically disordered proteins.

b. Magnification of the portion of the spectrum containing PG fragments. Uncross-linked (turquoise) and cross-linked (blue) muropeptides were color coded. The arrow indicates the donor→acceptor polarity in the cross-linked dimer. Sc and bb as DAP subscript correspond to the side chain and backbone amides, respectively.

c. Dose-dependent hydrolysis of nitrocefin by periplasmic extracts from *E. coli* cultures induced with increasing concentration of IPTG. Absorbance was monitored at 486 nm in PBS at 25 °C for 3 min.

d. Difference spectrum obtained by the subtraction of the non-induced *E. coli* pTRC99KΩ*kpc-2* from the spectrum obtained in panel a. Positive and negative contours are displayed in black and pale grey, respectively.

e. Superimposition of the 2D ^{1}H-^{15}N correlation spectra recorded at 37 °C for *E. coli* pTRC99KΩ*kpc-2* cells induced with 1 mM IPTG (difference spectrum from panel d in black, negative contours in pale grey), purified KPC-2 (grey), and a periplasmic extract from the *E. coli* pTRC99KΩ*kpc-2* strain induced with 1 mM IPTG (wheat). Purified KPC-2 was diluted in a periplasmic extract from a WT strain devoid of KPC-2 to minimize pH or buffer effects on amide resonance positions.

To further validate that the resonances observed in the processed spectrum (**Figure 1d**) derive indeed from KPC-2, we recorded a ^{1}H-^{15}N correlation spectrum on the purified enzyme, and observed that the 2 spectra overlap to a large extent (**Figure 1e**). As a prerequisite to *in situ* analyses, we also determined whether the KPC-2 spectrum recorded in intact bacteria actually corresponds to intracellular protein rather than protein released in the external medium following cell lysis. Toward this aim, we (1) optimized technical aspects of NMR sample preparation (extensive rinsing of cell pellet with PBS prior to NMR tube preparation), and (2) compared the result with a 2D ^{1}H-^{15}N correlation spectrum recorded on sample extracted from the periplasm of *E. coli* with induced KPC-2 production. An initial quick and efficient method of periplasm extraction based on Triton X-100 resulted in significant NMR peak broadening due to viscosity issues. In contrast, good quality spectra were obtained by using the osmotic-shock extraction procedure[18] (**Figure 1e**). In addition, (3) we also comparedspectra recorded in intact bacteria to an NMR spectrum recorded on purified KPC-2 in PBS buffer (**Figure S7a**), which revealed chemical shift perturbations (CSPs). Since amide resonances are highly sensitive to changes in the environment, we concluded that these CSPs reveal differences in the physicochemical conditions in the periplasm and in PBS. Finally, (4) we recorded 1D ^{1}H NMR spectra of external medium of the cells collected at time zero and 24 hours (**Figure S7b**). No NMR signals characteristic for KPC-2 were observed. These results collectively indicate that the KPC-2 spectra recorded on the agar embedded cells originate from the enzyme in its physiological periplasmic location.

In situ detection of avibactam binding to β-lactamase KPC-2

Our next objective was to monitor the inactivation of KPC-2 by the β-lactamase inhibitor avibactam in intact cells. Avibactam is known to reversibly form a covalent bond with the enzyme catalytic serine[28] (**Scheme 1**). We first validated the formation of a 1:1 KPC-2:avibactam complex with the purified β-lactamase (**Figure 2a**) and persistence of this complex over 48 hours (**Figure S8**). Observed NMR CSPs correlated well with the avibactam binding site previously identified by X-ray crystallography (PDB ID: 4ZBE)[29].

To effectively inhibit KPC-2 in cells, we first evaluated concentration of this enzyme in the periplasmic extract used for NMR experiments (~70 μM, **Figure S9a**). Since avibactam needs to cross the outer membrane though porins[30] to reach KPC-2 in the periplasm, we qualitatively probed KPC-2 inhibition in the range of increasing avibactam concentrations added to the cell culture using a nitrocefin assay (**Figure S9b**). It revealed that KPC-2 activity in *E. coli* cells decreases at the lowest tested concentration of avibactam (estimated 1:1 molar ratio) and is further diminished upon increasing avibactam concentration.

Having determined optimal *in-vitro* binding conditions of avibactam, we switched to in-cell NMR to follow KPC-2 inhibition directly in the bacterial periplasm. We compared 2D ^{1}H-^{15}N correlation spectra of KPC-2, both in the absence (apo form) and in the presence of avibactam (**Figure 2b**) resulting again in localized NMR chemical shift changes. The KPC-2 regions that are the most affected upon avibactam addition *in vitro* (**Figure 2c**) are also affected *in situ* (**Figure 2d**). Those regions are in agreement with the residues previously described as involved in the KPC-2/avibactam interaction[29,31]. Our in-cell NMR approach allowed the observation of β-lactamase inhibition directly under native conditions. In addition, a few CSP differences between *in vitro* and *in situ* conditions are observed. In particular additional CSPs observed for residues 108-114 (in a helix-loop-helix motif) and at the C-terminus (**Figure S10**) suggest some limited structural and dynamic changes upon avibactam binding that depend on the differences in *in vitro versus* periplasmic physicochemical conditions.

NMR differentiates mecillinam processing by KPC-2 and PBP2

After having shown that 2D ^{1}H-^{15}N NMR is a suitable method to monitor the inhibition of the KPC-2 β-lactamase inside the periplasm, we further investigated the competition between β-lactamase and PBP for β-lactam antibiotics. We chose mecillinam because this β-lactam selectively inactivates the essential PBP2 in contrast to most other β-lactams that target multiple PBPs. Mecillinam also has the advantage of yielding well resolved 1D ^{1}H NMR spectra for the intact drug and its hydrolysis product generated by KPC-2 (**Figure 3a** and **Figure S11**). NMR resonance assignments showed that the H_1 and methyl Me_5 and Me_6 protons of mecillinam were the most affected by β-lactam ring opening (**Figure 3b** and **Figure S11**)[32].

To evaluate the activity of KPC-2 in the periplasm, mecillinam was mixed with periplasmic extracts from cultures of *E. coli* strains harboring the vector pTRC99K (negative control) or its derivative encoding KPC-2. Recorded 1D ^{1}H NMR experiments revealed distinct spectral signatures for the two strains, consistent with hydrolysis of the β-lactam ring by KPC-2 (**Figure 3b**). Since the same peak pattern was observed for hydrolysis of mecillinam by purified KPC-2, we concluded that KPC-2 did hydrolyze mecillinam in periplasmic extracts.

We then investigated the KPC-2/PBP2 competition for mecillinam *in vitro* and *in situ*. Toward this aim, we mixed mecillinam with 1 molar equivalent of PBP2 *in vitro*, and observed that peaks of intact mecillinam disappeared from the ^{1}H spectrum without emergence of new signals corresponding to the hydrolyzed product. This indicates that mecillinam was covalently bound to PBP2, causing NMR signals to broaden and disappear from the spectrum. Thus, 1D ^{1}H NMR differentiates drug binding from drug hydrolysis in the reactions performed with PBP2 or KPC-2 alone, respectively (**Figure 3c**)[32]. Incubation of mecillinam with both PBP2 and KPC-2 in a 1:1

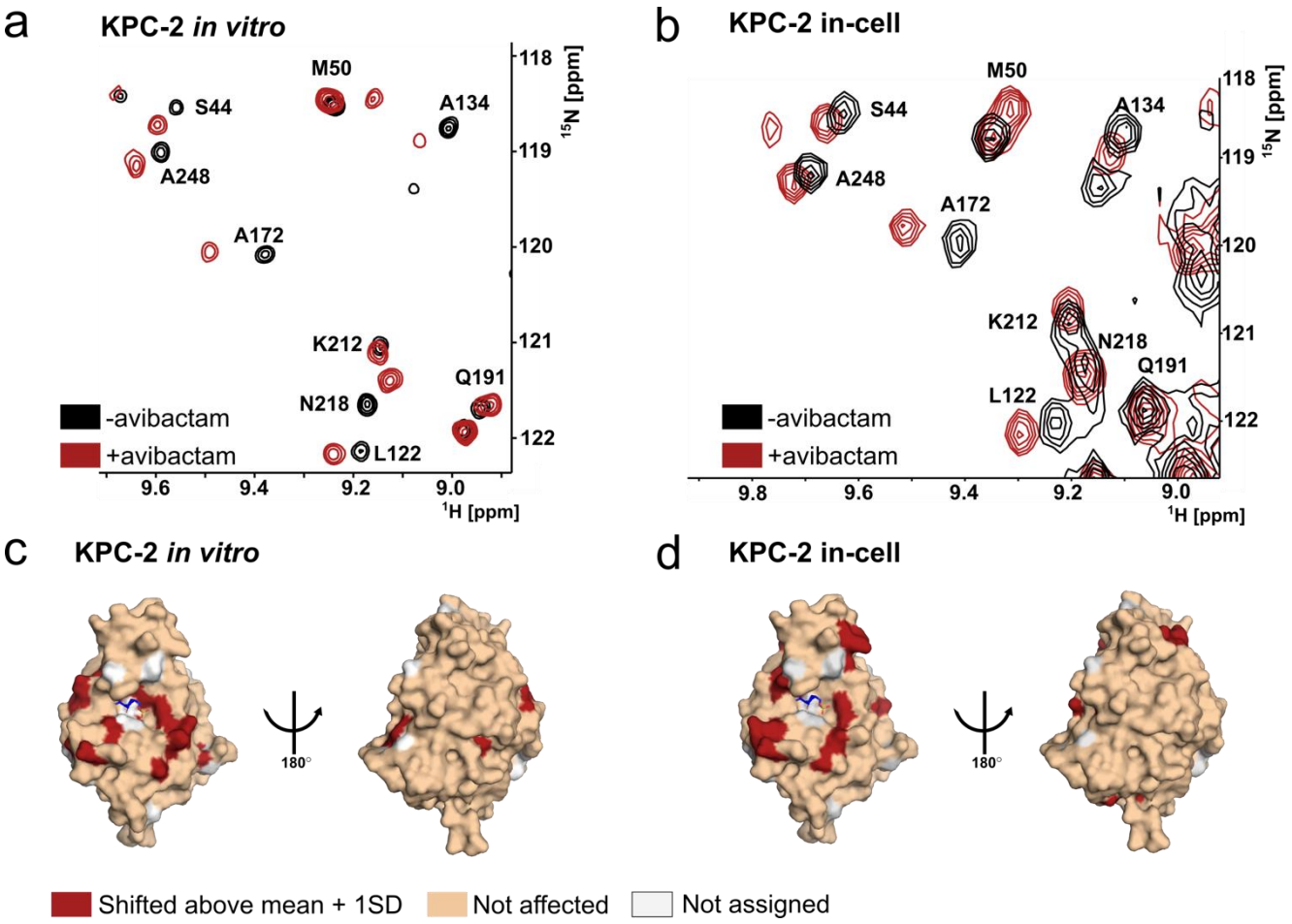

Figure 2 β-lactamase inhibition by avibactam *in situ*

a. Excerpt of the ^{1}H-^{15}N correlation spectra of ^{15}N-labelled KPC-2 recorded at 37 °C and pH 7.4. The experiment was conducted before (black) and after (crimson) addition of avibactam.

b. Excerpt of the ^{1}H-^{15}N correlation spectra of KPC-2 in ^{15}N-labelled *E. coli* cells at 37 °C. The color code is the same as in a.

c. Surface representation of KPC-2 (PDB ID: 4ZBE) indicating regions affected upon addition of avibactam *in vitro*. Avibactam is depicted as sticks. CSPs superior to 1 standard deviation (0.032 ppm) are colored in crimson. Unaffected and unassigned protein regions are colored in wheat and pale-grey, respectively.

d. Surface representation of KPC-2 regions affected upon *in situ* avibactam binding. CSPs superior to 1 standard deviation (0.031 ppm) are colored in crimson. The color code and avibactam representation are the same as in c.

protein-to-drug ratio for both enzymes resulted in the disappearance of ^{1}H signals corresponding to H_1, Me_5 and Me_6 of mecillinam. Thus, PBP2 outcompeted KPC-2 thereby preventing mecillinam hydrolysis. Increasing the KPC-2 to PBP2 molar ratio from 1 to 5 molar equivalent resulted in the appearance of ^{1}H NMR resonances corresponding to H_1 and Me_5 of hydrolyzed mecillinam. This observation indicates a shift from binding of mecillinam to PBP2 to hydrolysis of mecillinam by KPC-2 upon a five-fold increase in the KPC-2 to PBP2 ratio, which enabled KPC-2 to outcompete PBP2. Thus, the NMR approach successfully monitored the competition between two purified enzymes for a common substrate.

Tracking β-lactam hydrolysis *in situ*

We then asked whether drug binding and drug hydrolysis can be tracked inside bacterial cells using 1D ^{1}H NMR. While small molecules, such as β-lactams, are suitable targets for such an NMR study,[33] other cell components can negatively impact the quality of the spectrum, by contributing with broad and overlapping signals. To overcome this problem, we employed the $T_{1\rho}$ filtering method, which separates the present molecular species based on their transversal relaxation rates[34]. As a result, broadened NMR signals of high molecular weight molecules are largely suppressed, whereas those from small molecules, such as mecillinam, are mostly retained. Another challenge of in-cell NMR experiments is to ensure that the monitored reactions actually and uniquely take place inside the cells.

This is particularly problematic for studies concerning enzymes, which are effective at very low (nanomolar) concentrations. Periplasmic components are potentially released to the external environment due to cell lysis occurring during both sample preparation and experiment recording. We estimated that ~3 nM of KPC-2 was released from the *E. coli* culture during the NMR data recording time of about 1.5 hours (**Figure S12a**). To remove external KPC-2, all mecillinam hydrolysis assays were performed in the presence of pepsin, a broad-range protease. We evaluated that the pepsin concentration required to inactivate released KPC-2 was 4 mg/ml (**Figure S12b**), and confirmed that such an extracellular concentration of pepsin was not harmful for the cells (**Figure S12c**). These results indicate that the monitored reaction of mecillinam hydrolysis by KPC-2 mostly took place inside the periplasm.

1D ^{1}H NMR spectra of pepsin and mecillinam revealed that their signals do not overlap (**Figure S13**), which allows monitoring of the hydrolysis reaction. Within a few minutes after mixing cells with mecillinam, we observed peak shifts and line broadening for mecillinam resonances (for H_1, H_2, H_3, Me_5 and Me_6; **Figure 3d**), and the appearance of new peaks corresponding to hydrolyzed mecillinam.

In the studied system PBP2 is in its physiological concentration range, which is below the detection limit for NMR (< 20 µM). Therefore, we cannot observe the disappearance of NMR signals due to mecillinam binding to PBP2. Appearance of the hydrolyzed products indicates that KPC-2 outcompetes PBP2 for mecillinam. Therefore, KPC-2 potentially compensates its low affinity for mecillinam with a high local abundance in the native context.

Inhibition of β-lactam hydrolysis *in situ*

Our last objective was to monitor the *in situ* inhibition of KPC-2 activity by pre-incubating cells with avibactam at a 10:1 avibactam:KPC-2 molar ratio prior to the addition of mecillinam (**Figure 3e**). This experiment revealed NMR signals corresponding to both authentic and hydrolyzed mecillinam. Based on comparison of NMR peak intensities determined on the resonances of the mecillinam hydrolysis product, the pre-treatment with avibactam partially (*ca.* 50%) prevented mecillinam hydrolysis under the assay conditions (**Figure S14**). This result is in agreement with the nitrocefin hydrolysis assay, which also revealed a *ca.* 50% decrease in the formation of the β-lactam hydrolysis product upon pre-treatment of bacterial cells with avibactam (**Figure S9b**). Residual β-lactamase activity could be accounted for by the fact that avibactam reversibly binds to KPC-2[28,35], leading to an equilibrium between the active and avibactam-inactivated forms of the β-lactamase.

CONCLUSION

The development of more effective treatments against drug-resistant pathogens requires advanced tools allowing to monitor their action in native conditions. In this work, we comprehensively characterized β-lactams in the bacterial periplasm, using a set of 1D and 2D in-cell NMR experiments. To ensure that the processes are observed in intact cells and not after lysis, a particular effort was made to stabilize the cells in agar medium, while maintaining the optimal sensitivity of the experiments. Observation and monitoring of drug status by 1D NMR methods was optimized, using size-dependent filters to reduce signals from larger molecules. We ensured the lack of externally released enzymes by washing the cells and using the external addition of pepsin, a non-specific peptidase. We demonstrated that periplasmic β-lactamases can be observed with good sensitivity and that the evolution of drug/enzyme complexes can be followed directly in cells or in periplasmic extracts obtained with extraction methods compatible with NMR experiments.

This approach is particularly useful to characterize new inhibitors/drugs targeting periplasmic components, which includes (1) monitoring of drug transformation and/or binding, (2) determination of the drug binding sites on protein target, and (3) evaluation of their effect on the performed enzymatic reactions in the cellular context. In-cell NMR that does not require purification and selective tagging of the studied enzymes, allows the evaluation of drug efficacy directly in their native environment. In addition, it offers an opportunity to connect these observations with the presence of specific PG turnover products, physiological signals boosting β-lactamases expression[21]. Following the variation of their concentration and composition upon antimicrobial exposure could therefore serve as a hallmark of the cell fitness[36].

Using KPC-2 as an example, we observed differences between *in vitro* and *in vivo* conditions (inhibitor binding pattern [**Figure 2c, d**]) proving usefulness of selected *in situ* approach. Therefore, the major novelty of the presented work is the comprehensive picture of reactions monitored directly in the bacterial periplasm at residue resolution. The experimental strategies presented here can be easily transferred to the investigation of new drugs targeting different bacterial periplasmic components.

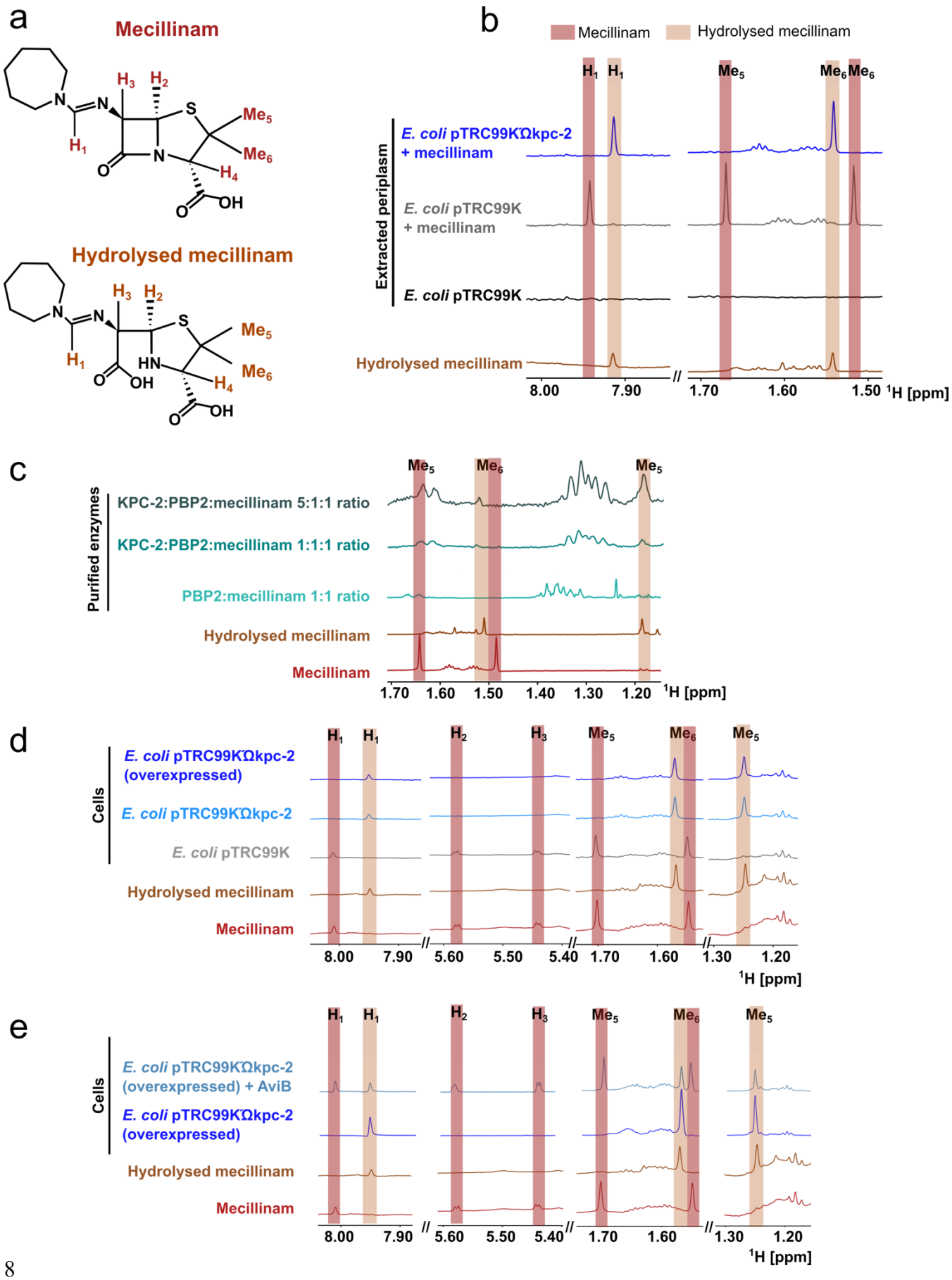
a
Mecillinam
Hydrolysed mecillinam
b
Mecillinam
Hydrolysed mecillinam
Extracted periplasm
E. coli pTRC99KΩkpc-2 + mecillinam
E. coli pTRC99K + mecillinam
E. coli pTRC99K
Hydrolysed mecillinam
1H [ppm]
c
Purified enzymes
KPC-2:PBP2:mecillinam 5:1:1 ratio
KPC-2:PBP2:mecillinam 1:1:1 ratio
PBP2:mecillinam 1:1 ratio
Hydrolysed mecillinam
Mecillinam
1H [ppm]
d
Cells
E. coli pTRC99KΩkpc-2 (overexpressed)
E. coli pTRC99KΩkpc-2
E. coli pTRC99K
Hydrolysed mecillinam
Mecillinam
1H [ppm]
e
Cells
E. coli pTRC99KΩkpc-2 (overexpressed) + AviB
E. coli pTRC99KΩkpc-2 (overexpressed)
Hydrolysed mecillinam
Mecillinam
1H [ppm]

Figure 3 β-lactamase hydrolyses mecillinam *in-situ*

a. Chemical structures of mecillinam and its hydrolyzed form. Protons, for which NMR resonances were followed during the hydrolysis reaction, were marked in red for mecillinam and in brown for its hydrolyzed form.[32]

b. 1D ^{1}H $T_{1\rho}$-filtered spectra recorded with a spinlock amplitude of 1.7 kHz and a duration of 50 ms at pH 8.0 and 25 °C for the incubation of mecillinam with periplasmic extracts from *E. coli* strains harboring the vector pTRC99K (no KPC-2 production) or the recombinant plasmid pTRC99KΩ*kpc-2* (KPC-2 production). The numbering of mecillinam protons and the color code follow the ones presented in panel a.

c. Experiments recorded as described in panel b with KPC-2, PBP2, and mecillinam at 1:1:1 and 5:1:1 molar ratios. Experiments were recorded in 50 mM phosphate buffer, 150 mM NaCl pH 7.0.

d. Experiments recorded as described in panel b for *E. coli* pTRC99K and pTRC99KΩ*kpc-2* cells mixed with mecillinam and embedded in 0.5% agar PBS pH 7.4. The experiments were performed in the presence of 4 mg/ml pepsin.

e. Experiments recorded as in panel d for *E. coli* pTRC99KΩ*kpc-2* cells pre-incubated with avibactam (AviB) at 700 μM.

ASSOCIATED CONTENT

Additional experimental details, materials, and methods (DOC). This material is available free of charge via the Internet at http://pubs.acs.org.

AUTHOR INFORMATION

Corresponding Author

* Email: jean-pierre.simorre@ibs.fr

Present Addresses

†Yale University Boyer Center for Molecular Medicine, New Haven, CT, 06536, United States

Author Contributions

All authors have given approval to the final version of the manuscript.

Funding Sources

This research is part of Narrow Spectrum Antibiotics to Fight the Emergence of Bacterial Resistance project (NASPEC, 20-PAMR-0007) founded by Agence Nationale de la Recherche. This work used the platforms of the Grenoble Instruct-ERIC center (ISBG; UAR 3518 CNRSCEA-UGA-EMBL) within the Grenoble Partnership for Structural Biology (PSB), supported by FRISBI (ANR-10-INBS-0005-02) and GRAL, financed within the University Grenoble Alpes graduate school (Ecoles Universitaires de Recherche) CBH-EUR-GS (ANR-17-EURE-0003). Financial support from the IR INFRANALYTICS FR2054 for conducting the research is gratefully acknowledged.

Notes

The authors declare no competing financial interest.

ACKNOWLEDGMENT

Authors would like to thank Dr. Bernhard Brutscher for conscious reading of the manuscript.

ABBREVIATIONS

PG, peptidoglycan; *N*-Acetylmuramic acid, Mur*N*Ac; *N*-Acetylglucosamine, Glc*N*Ac; anhMur*N*Ac, 1,6-anhydro-*N*-acetylmuramic acid**;** IDPs, intrinsically disordered proteins; CSPs, Chemical Shift Perturbations; PBPs, penicillin-binding proteins; NMR, nuclear magnetic resonance.

REFERENCES

(1) Darby, E. M.; Trampari, E.; Siasat, P.; Gaya, M. S.; Alav, I.; Webber, M. A.; Blair, J. M. A. Molecular Mechanisms of Antibiotic Resistance Revisited. *Nat. Rev. Microbiol.* **2023**, *21* (5), 280–295. https://doi.org/10.1038/s41579-022-00820-y.

(2) D'Souza, A. W.; Potter, R. F.; Wallace, M.; Shupe, A.; Patel, S.; Sun, X.; Gul, D.; Kwon, J. H.; Andleeb, S.; Burnham, C.-A. D.; Dantas, G. Spatiotemporal Dynamics of Multidrug Resistant Bacteria on Intensive Care Unit Surfaces. *Nat. Commun.* **2019**, *10* (1), 4569. https://doi.org/10.1038/s41467-019-12563-1.

(3) Carattoli, A. Plasmids in Gram Negatives: Molecular Typing of Resistance Plasmids. *Int. J. Med. Microbiol.* **2011**, *301* (8), 654–658. https://doi.org/10.1016/j.ijmm.2011.09.003.

(4) ur Rahman, S.; Ali, T.; Ali, I.; Khan, N. A.; Han, B.; Gao, J. The Growing Genetic and Functional Diversity of Extended Spectrum Beta-Lactamases. *BioMed Res. Int.* **2018**, *2018*, e9519718. https://doi.org/10.1155/2018/9519718.

(5) Sauvage, E.; Kerff, F.; Terrak, M.; Ayala, J. A.; Charlier, P. The Penicillin-Binding Proteins: Structure and Role in Peptidoglycan Biosynthesis. *FEMS Microbiol. Rev.* **2008**, *32* (2), 234–258. https://doi.org/10.1111/j.1574-6976.2008.00105.x.

(6) Mojica, M. F.; Rossi, M.-A.; Vila, A. J.; Bonomo, R. A. The Urgent Need for Metallo-β-Lactamase Inhibitors: An Unattended Global Threat. *Lancet Infect. Dis.* **2022**, *22* (1), e28–e34. https://doi.org/10.1016/S1473-3099(20)30868-9.

(7) Tooke, C. L.; Hinchliffe, P.; Bragginton, E. C.; Colenso, C. K.; Hirvonen, V. H. A.; Takebayashi, Y.; Spencer, J. β-Lactamases and β-Lactamase Inhibitors in the 21st Century. *J. Mol. Biol.* **2019**, *431* (18), 3472–3500. https://doi.org/10.1016/j.jmb.2019.04.002.

(8) Hunashal, Y.; Kumar, G. S.; Choy, M. S.; D'Andréa, É. D.; Da Silva Santiago, A.; Schoenle, M. V.; Desbonnet, C.; Arthur, M.; Rice, L. B.; Page, R.; Peti, W. Molecular Basis of β-Lactam Antibiotic Resistance of ESKAPE Bacterium *E. Faecium* Penicillin Binding Protein PBP5. *Nat. Commun.* **2023**, *14* (1), 4268. https://doi.org/10.1038/s41467-023-39966-5.

(9) Taguchi, A.; Welsh, M. A.; Marmont, L. S.; Lee, W.; Sjodt, M.; Kruse, A. C.; Kahne, D.; Bernhardt, T. G.; Walker, S. FtsW Is a Peptidoglycan Polymerase That Is Functional Only in Complex with Its Cognate Penicillin-Binding Protein. *Nat. Microbiol.* **2019**, *4* (4), 587–594. https://doi.org/10.1038/s41564-018-0345-x.

(10) Catherwood, A. C.; Lloyd, A. J.; Tod, J. A.; Chauhan, S.; Slade, S. E.; Walkowiak, G. P.; Galley, N. F.; Punekar, A. S.; Smart, K.; Rea, D.; Evans, N. D.; Chappell, M. J.; Roper, D. I.; Dowson, C. G. Substrate and Stereochemical Control of Peptidoglycan Cross-Linking by Transpeptidation by *Escherichia coli* PBP1B. *J. Am. Chem. Soc.* **2020**, *142* (11), 5034–5048. https://doi.org/10.1021/jacs.9b08822.

(11) Qiao, Y.; Srisuknimit, V.; Rubino, F.; Schaefer, K.; Ruiz, N.; Walker, S.; Kahne, D. Lipid II Overproduction Allows Direct Assay of Transpeptidase Inhibition by β-Lactams. *Nat. Chem. Biol.* **2017**, *13* (7), 793–798. https://doi.org/10.1038/nchembio.2388.

(12) Triboulet, S.; Edoo, Z.; Compain, F.; Ourghanlian, C.; Dupuis, A.; Dubée, V.; Sutterlin, L.; Atze, H.; Etheve-Quelquejeu, M.; Hugonnet, J.-E.; Arthur, M. Tryptophan Fluorescence Quenching in β-Lactam-Interacting Proteins Is Modulated by the Structure of Intermediates and Final Products of the Acylation Reaction. *ACS Infect. Dis.* **2019**, *5* (7), 1169–1176. https://doi.org/10.1021/acsinfecdis.9b00023.

(13) Schur, F. K. Toward High-Resolution in Situ Structural Biology with Cryo-Electron Tomography and Subtomogram Averaging. *Curr. Opin. Struct. Biol.* **2019**, *58*, 1–9. https://doi.org/10.1016/j.sbi.2019.03.018.

(14) Hale, O. J.; Cooper, H. J. In Situ Mass Spectrometry Analysis of Intact Proteins and Protein Complexes from Biological Substrates. *Biochem. Soc. Trans.* **2020**, *48* (1), 317–326. https://doi.org/10.1042/BST20190793.

(15) Jing, Y.; Zhang, C.; Yu, B.; Lin, D.; Qu, J. Super-Resolution Microscopy: Shedding New Light on In Vivo Imaging. *Front. Chem.* **2021**, *9* (746900). https://doi.org/10.3389/fchem.2021.746900.

(16) Luchinat, E.; Banci, L. In-Cell NMR: A Topical Review. *IUCrJ* **2017**, *4* (2), 108–118. https://doi.org/10.1107/S2052252516020625.

(17) Luchinat, E.; Banci, L. In-Cell NMR: Recent Progresses and Future Challenges. *Rendiconti Lincei Sci. Fis. E Nat.* **2023**, *34* (3), 653–661. https://doi.org/10.1007/s12210-023-01168-y.

(18) Theillet, F.-X.; Luchinat, E. In-Cell NMR: Why and How? *Prog. Nucl. Magn. Reson. Spectrosc.* **2022**, *132–133*, 1–112. https://doi.org/10.1016/j.pnmrs.2022.04.002.

(19) Cho, H.; Uehara, T.; Bernhardt, T. G. Beta-Lactam Antibiotics Induce a Lethal Malfunctioning of the Bacterial Cell Wall Synthesis Machinery. *Cell* **2014**, *159* (6), 1300–1311. https://doi.org/10.1016/j.cell.2014.11.017.

(20) Voedts, H.; Kennedy, S. P.; Sezonov, G.; Arthur, M.; Hugonnet, J.-E. Genome-Wide Identification of Genes Required for Alternative Peptidoglycan Cross-Linking in Escherichia Coli Revealed Unexpected Impacts of β-Lactams. *Nat. Commun.* **2022**, *13* (1), 7962. https://doi.org/10.1038/s41467-022-35528-3.

(21) Zeng, X.; Lin, J. Beta-Lactamase Induction and Cell Wall Metabolism in Gram-Negative Bacteria. *Front. Microbiol.* **2013**, *4*, 128. https://doi.org/10.3389/fmicb.2013.00128.

(22) Favier, A.; Brutscher, B. Recovering Lost Magnetization: Polarization Enhancement in Biomolecular NMR. *J. Biomol. NMR* **2011**, *49* (1), 9–15. https://doi.org/10.1007/s10858-010-9461-5.

(23) Atze, H.; Liang, Y.; Hugonnet, J.-E.; Gutierrez, A.; Rusconi, F.; Arthur, M. Heavy Isotope Labeling and Mass Spectrometry Reveal Unexpected Remodeling of Bacterial Cell Wall Expansion in Response to Drugs. *eLife* **2022**, *11*, e72863. https://doi.org/10.7554/eLife.72863.

(24) Fontana, C.; Widmalm, G. Primary Structure of Glycans by NMR Spectroscopy. *Chem. Rev.* **2023**, *123* (3), 1040–1102. https://doi.org/10.1021/acs.chemrev.2c00580.

(25) Weaver, A. I.; Alvarez, L.; Rosch, K. M.; Ahmed, A.; Wang, G. S.; Van Nieuwenhze, M. S.; Cava, F.; Dörr, T. Lytic Transglycosylases Mitigate Periplasmic Crowding by Degrading Soluble Cell Wall Turnover Products. *eLife* **2022**, *11*, e73178. https://doi.org/10.7554/eLife.73178.

(26) Sciolino, N.; Burz, D. S.; Shekhtman, A. In-Cell NMR Spectroscopy of Intrinsically Disordered Proteins. *PROTEOMICS* **2019**, *19* (6), 1800055. https://doi.org/10.1002/pmic.201800055.

(27) Barbieri, L.; Luchinat, E.; Banci, L. Characterization of Proteins by In-Cell NMR Spectroscopy in Cultured Mammalian Cells. *Nat. Protoc.* **2016**, *11* (6), 1101–1111. https://doi.org/10.1038/nprot.2016.061.

(28) Ehmann, D. E.; Jahić, H.; Ross, P. L.; Gu, R.-F.; Hu, J.; Kern, G.; Walkup, G. K.; Fisher, S. L. Avibactam Is a Covalent, Reversible, Non–β-Lactam β-Lactamase Inhibitor. *Proc. Natl. Acad. Sci.* **2012**, *109* (29), 11663–11668. https://doi.org/10.1073/pnas.1205073109.

(29) Krishnan, N. P.; Nguyen, N. Q.; Papp-Wallace, K. M.; Bonomo, R. A.; van den Akker, F. Inhibition of Klebsiella β-Lactamases (SHV-1 and KPC-2) by Avibactam: A Structural Study. *PloS One* **2015**, *10* (9), e0136813. https://doi.org/10.1371/journal.pone.0136813.

(30) Zhao, S.; Adamiak, J. W.; Bonifay, V.; Mehla, J.; Zgurskaya, H. I.; Tan, D. S. Defining New Chemical Space for Drug Penetration into Gram-Negative Bacteria. *Nat. Chem. Biol.* **2020**, *16* (12), 1293–1302. https://doi.org/10.1038/s41589-020-00674-6.

(31) King, D. T.; King, A. M.; Lal, S. M.; Wright, G. D.; Strynadka, N. C. J. Molecular Mechanism of Avibactam-Mediated β-Lactamase Inhibition. *ACS Infect. Dis.* **2015**, *1* (4), 175–184. https://doi.org/10.1021/acsinfecdis.5b00007.

(32) Hinchliffe, P.; Calvopiña, K.; Rabe, P.; Mojica, M. F.; Schofield, C. J.; Dmitrienko, G. I.; Bonomo, R. A.; Vila, A. J.; Spencer, J. Interactions of Hydrolyzed β-Lactams with the L1 Metallo-β-Lactamase: Crystallography Supports Stereoselective Binding of Cephem/Carbapenem Products. *J. Biol. Chem.* **2023**, *299* (5). https://doi.org/10.1016/j.jbc.2023.104606.

(33) Ma, J.; McLeod, S.; MacCormack, K.; Sriram, S.; Gao, N.; Breeze, A. L.; Hu, J. Real-Time Monitoring of New Delhi Metallo-β-Lactamase Activity in Living Bacterial Cells by ^{1}H NMR Spectroscopy. *Angew. Chem. Int. Ed.* **2014**, *53* (8), 2130–2133. https://doi.org/10.1002/anie.201308636.

(34) Piersanti, E.; Rezig, L.; Tranchida, F.; El-Houri, W.; Abagana, S. M.; Campredon, M.; Shintu, L.; Yemloul, M. Evaluation of the Rotating-Frame Relaxation ($T_{1\rho}$) Filter and Its Application in Metabolomics as an Alternative to the Transverse Relaxation (T_2) Filter. *Anal. Chem.* **2021**, *93* (25), 8746–8753. https://doi.org/10.1021/acs.analchem.0c05251.

(35) Ourghanlian, C.; Soroka, D.; Arthur, M. Inhibition by Avibactam and Clavulanate of the β-Lactamases KPC-2 and CTX-M-15 Harboring the Substitution N132G in the Conserved SDN Motif. *Antimicrob. Agents Chemother.* **2017**, *61* (3), 10.1128/aac.02510-16. https://doi.org/10.1128/aac.02510-16.

(36) Jacobs, C.; Frère, J.-M.; Normark, S. Cytosolic Intermediates for Cell Wall Biosynthesis and Degradation Control Inducible β-Lactam Resistance in Gram-Negative Bacteria. *Cell* **1997**, *88* (6), 823–832. https://doi.org/10.1016/S0092-8674(00)81928-5.

Table of Content :